



Diagnostic Performance of Diffusion-Weighted MRI and FDG PET/CT for Detecting the Local Recurrence of Head and Neck Squamous Cell Carcinoma

Baş-boyun Skuamöz Hücreli Karsinomlarında Lokal Nüksün Saptanmasında Difüzyon Ağırlıklı MR ve FDG PET/BT'nin Tanısal Performansı

İbrahim İlker Öz¹, İsmail Şerifoğlu¹, Yavuz Sami Salıhoğlu³, Murat Damar², Aykut Erdem Dinç², Rabiye Uslu³, Mustafa Çağatay Büyükuysal⁴, Oktay Erdem¹

Abstract / Öz

Objective: To compare the efficacy between diffusion-weighted magnetic resonance imaging (DW-MRI) and positron emission tomography/computed tomography (PET/CT) in detecting the local recurrence of head and neck squamous cell carcinoma (HNSCC) following treatment in the same patient group.

Methods: Twenty-three patients who had biopsy-proven HNSCC were enrolled. All patients were treated with radiotherapy and followed up with MRI and PET/CT. The median delay times between radiotherapy and MRI and between MRI and FDG PET/CT were 71 days (range: 43–98 days) and 75 days (range: 44–103 days), respectively. Diffusion-weighted single-shot echo planar imaging was performed before contrast injection at b values of 0 and 1000 s/mm². PET/CT images were acquired after the administration of 3.7 MBq/kg of fluorine-18-fluorodeoxyglucose, and the images were acquired 1 h later.

Results: The apparent diffusion coefficient (ADC) mean values of the recurrence group were significantly lower than those of the post-treatment changes group (0.773 vs. 1.588×10⁻³ mm²/s, respectively; p<0.001). The standardized uptake value (SUV)_{max} values of the recurrence group were significantly higher than those of the post-treatment changes group (15.642 vs. 4.508, respectively; p<0.001). There was no significant correlation between ADC_{mean} and SUV_{max} values of recurrence (r=0.341; p=0.278), whereas there was a negative correlation between ADC_{mean} and SUV_{max} values of the post-treatment changes (r=-0.691; p=0.019).

Conclusion: PET/CT and DW-MRI are effective methods for distinguishing recurrence from post-treatment changes. Follow-up should begin with DW-MRI, and in patients with a suspicion of recurrence, PET-CT should be added to the follow-up protocol.

Keywords: Head and neck cancer, diffusion weighted imaging, apparent diffusion coefficient, positron emission tomography/computed tomography, standardized uptake value

Amaç: Baş-boyun skuamöz hücreli karsinom (SCC) lokal nüksün saptanmasında difüzyon ağırlıklı manyetik rezonans görüntüleme (DA-MRG) ve pozitron emisyon tomografi/bilgisayarlı tomografi (PET/BT) etkinliğini karşılaştırmak.

Yöntemler: Baş-boyun SCC tanısı biyopsi ile kanıtlanmış ve radyoterapi ile tedavi edilen 23 hasta çalışmaya dahil edildi. Takipte tüm hastalardan MRG ve PET/BT incelemesi yapıldı. Tedavinin tamamlanması ile MR ve PET/BT incelemeleri arasındaki ortalama süre sırasıyla 70,30 gün (aralık 43-98) ve 76,34 gün (aralık 44-103) idi. Difüzyon ağırlıklı single-shot eko planar görüntüleme 0 ve 1000 sn/mm² b değerlerinde kontrast enjeksiyonundan önce yapıldı. PET/BT görüntüleri flor-18-fluorodeoksiglukoz (3.7 MBq/kg) verilmesinden 1 saat sonra görüntüler elde edildi.

Bulgular: Nüks saptanan hastalarda ADC_{ortalama} değerleri saptanmayan hastalarla karşılaştırıldığında istatistiksel olarak anlamlı derecede düşük bulunmuştur (0,773'e karşı 1,588 x10-3/mm² sırasıyla, p<0,001). Nüks saptanan hastalarda SUV_{max} değerleri saptanmaya hastalara göre istatistiksel olarak anlamlı derecede yüksek bulundu (15,642' karşı 4,508 sırasıyla; p<0,001). Nüks saptanan hastalarda ADC_{ortalama} ve SUV_{max} değerleri arasında anlamlı bir korelasyon izlenmedi (p=0,278, r=0,341). Nüks saptanmayan hastalarda ADC_{ortalama} ve SUV_{max} değerleri arasında negatif korelasyon saptandı (p=0,019, r=-0,691).

Sonuç: PET/BT ve DAG-MRG baş-boyun SCC hastalarında tedavi sonrası nüksü saptamada etkin yöntemlerdir. Baş-Boyun SCC hastaları tedavi sonrası DAG-MRG ile takip edilebilir ve nüks şüphesi olan hastalarda PET-BT takip protokolüne eklenebilir.

Anahtar Kelimeler: Baş ve boyun kanseri; difüzyon ağırlıklı görüntüleme, görünür difüzyon katsayısı, pozitron emisyon tomografisi/bilgisayarlı tomografi, standardize tutulum değeri

Introduction

For patients with head and neck squamous cell carcinoma (HNSCC), multidisciplinary treatment involving surgery, radiotherapy, and/or chemotherapy improves survival and quality of life (1, 2). Despite aggressive combined management, locoregional recurrence is observed in approximately 40% of patients (3). Physical examination after treatment can be compromised by post-treatment changes, as surgical intervention can change the normal anatomy and radiotherapy can cause edema, inflammation, fibrosis, and necrosis (4). Particularly in the early stages of treatment, post-treatment follow-up imaging is also a challenge. Differentiation of post-treatment changes from a recurrence of HNSCC is generally not possible on computed tomography (CT) or magnetic resonance imaging (MRI); recurrent tumors and post-treatment changes may show similar appearances on routine MRI. After contrast administration, mass-like enhancement of post-treatment changes may mimic recurrence (1). Conversely, some recurrent tumors do not show enhancements, and thus, they cannot be distinguished from post-treatment changes (5).

Diffusion-weighted MRI (DW-MRI) is sensitive to the randomized (Brownian) motion of water molecules. This imaging technique uses two opposite gradients of similar strength along a particular diffusion direction. The first gradient stimulates dephasing, and the second gradient will completely rephase all stationary molecules. Consequently, the movement of protons in living tissues results in incomplete rephasing and is then converted into a decrease in the signal intensity on the resulting image (6, 7). The apparent diffusion coefficient (ADC) is a quantitative value associ-

¹Department of Radiology, Bülent Ecevit University School of Medicine, Zonguldak, Türkiye

²Department of Otolaryngology, Bülent Ecevit University School of Medicine, Zonguldak, Türkiye

³Department of Nuclear Medicine, Bülent Ecevit University School of Medicine, Zonguldak, Türkiye

⁴Department of Medical Statistics, Bülent Ecevit University School of Medicine, Zonguldak, Türkiye

Address for Correspondence

Yazışma Adresi:

İbrahim İlker Öz

E-mail: ilkeroz@yahoo.com

Received/Geliş Tarihi:
11.02.2016

Accepted/Kabul Tarihi:
31.03.2016

© Copyright 2016 by Available online at
www.istanbulmedicaljournal.org

© Telif Hakkı 2016 Makale metnine
www.istanbultipdergisi.org web sayfasından
ulaşılabilir.

ated with the amount and speed of proton movement within the tissue and calculated from the DW-MRI (7, 8). In living tissues, cell size, density, and integrity affect diffusivity.

Fluorodeoxyglucose (FDG) positron emission tomography (PET)/CT is a functional imaging method that measures increased cellular glucose metabolism as expressed by the standardized uptake value (SUV) (9). At the tissue level, FDG uptake is correlated with the number of viable tumor cells and their metabolic activities (8). SUV_{max} is the most common quantitative measurement because the value is independent of the observer and the size of the selected region of interest (ROI) (10).

Many studies have shown the advantages of DW-MRI or PET/CT for distinguishing recurrent tumors from post-treatment changes in head and neck cancers (1, 2, 4, 9). However, few studies have investigated the diagnostic performance of DW-MRI and PET-CT in the same patients with head and neck cancers (8, 11). Moreover, there have been no reports on the diagnostic performance of DW-MRI and PET-CT in distinguishing between recurrence and post-treatment changes in the same patient group. Therefore, in the present study, we compared ADC_{mean} and SUV_{max} values to define their diagnostic significance in the detection of recurrence in HNSCC within the same patient group.

Methods

This retrospective study was approved by the Bulent Ecevit University Clinical Research Ethics Committee. Informed consent was obtained from all individuals. Inclusion criteria consisted of adult patients with histologically proven HNSCC, who had been treated with radiotherapy, undergone an endoscopic examination, and received both DWI-MRI and FDG PET/CT. From a computerized search of the PACS archives and medical records of our institution from November 2011 to January 2014, we identified 32 adult patients with histologically proven HNSCC who had been treated with radiotherapy. We obtained the pathological diagnosis of all of these patients by reviewing the medical records at our institution. All patients who met the following criteria were included in this study: 1) patients who had undergone an endoscopic examination after radiotherapy; and 2) patients who received both DWI-MRI and FDG PET/CT. Three patients were excluded due to lesions that were <1 cm in size, which does not allow ADC measurements. Six patients were excluded because they did not have a biopsy-proven diagnosis of recurrence or post-treatment changes. Due to possible biopsy sampling errors, post-treatment changes were also followed up for a minimum of 6 months. No changes or decrease in the size of the lesions on MR images and no other support for recurrence in the clinical examination were accepted as post-treatment changes. Three patients had poor DW-MRI quality from breathing and swallowing artifacts. These patients were not excluded because the MR test characteristics would have been artificially elevated (i.e., biased for higher accuracy). Finally, 23 patients who had a biopsy-proven diagnosis after treatment (3 women and 20 men) with a median age of 65 years (range: 19–81 years) were included in the study. All patients were treated with radiotherapy: alone (n=9), after surgical intervention (n=6), or simultaneously with chemotherapy (n=8). The median delay times between radiotherapy and MRI and between MRI and FDG PET/CT were 71 days (range: 43–98 days) and 75 days (range: 44–103 days), respectively. The median

delay time between the two examinations was 6 days (range: 1–12 days). The median follow-up duration for the patients was 14.5 months (range: 7–26.7 months).

MRI and PET/CT Imaging Techniques

A 1.5-Tesla system (Intera Master Gyroscan; Philips Medical Systems, Best, the Netherlands) with a head/neck coil was used for MRI. Routine MRI protocols were used for all patients, including transverse T1-weighted turbo spin-echo (TSE) (TR/TE=430/12 ms) and T2-weighted turbo spin-echo (TSE) (TR/TE=6925/120 ms) sequences with or without fat suppression and a slice thickness of 6 mm, slice gap of 0.6 mm, field of view of 23×25 cm, and a matrix size of 228×512.

Diffusion-weighted single-shot echo planar imaging was performed before the contrast injection at b values 0 and 1000 s/mm² with the following parameters: TR/TE=4000–4280/94–110 ms, a field of view of 23×28 cm, matrix size of 94×160, slice thickness of 6 mm, slice gap of 1.2 mm, and bandwidth of 2.137 kHz. Spectral presaturation with inversion recovery (SPIR) was used for fat suppression. We did not use any antisusceptibility devices on the head and neck to decrease susceptibility artifacts, and respiratory triggering and cardiac gating were not used.

Next, we obtained T1-weighted turbo spin-echo (TR/TE=430–606/12 ms) in the transverse, sagittal, and coronal planes after an intravenous injection of gadopentetate dimeglumine (Magnevist; Bayer Pharma AG, Berlin, Germany) was administered in all patients. The SPIR for fat suppression had a slice thickness of 6 mm, slice gap of 0.6 mm, field of view of 23×25 cm, and matrix size of 190×512.

PET/CT images were acquired using an integrated PET/CT scanner (Gemini TF PET/CT 16-slice; Philips Medical Systems). Patients fasted for at least 6 h before undergoing the scan, 3.7 MBq/kg of fluorine-18-FDG was administered, and images were acquired 1 h later. Glucose levels were measured in all patients before the examination, with a cutoff limit of 8.3 mmol/L (150 mg/dL). The PET scan was performed with a 1.5 min per bed position, from the vertex to the proximal thigh. CT data acquisition for attenuation correction was performed using the following parameters: 120 kV, 150 mAs, 16×1.5 collimation slice, pitch=0.81, and 0.5 s per rotation. PET images were reconstructed using the Gemini TF's default reconstruction algorithm (BLOB-OS-TF; a 3-dimensional ordered-subset iterative time-of-flight reconstruction technique using three iterations, 33 subsets, and a voxel size of 4×4×4 mm) with a slice thickness of 5 mm. SUV was calculated using the standard formula: $SUV = \text{measured radioactivity concentration from tissue (Bq/g)} / \text{injected radioactivity dose (Bq)/patient's body weight (g)}$.

MRI and PET/CT Imaging Analysis

Reviewers were blinded to clinical data and histopathology. Images were evaluated by two reviewers: 1) a radiologist with 6 years of experience in head and neck MRI and 2) a nuclear medicine specialist with 5 years of experience in PET/CT imaging. The reviewers were free to use any window setting and multi-planar evaluation to optimize the visualization of the lesions. Images used to calculate ADC_{mean} and SUV_{max} values were selected in consultation with the authors.

A computer program included in the Philips Extended MR Workspace (version 2.6.3.2; Philips Medical Systems) was used for the

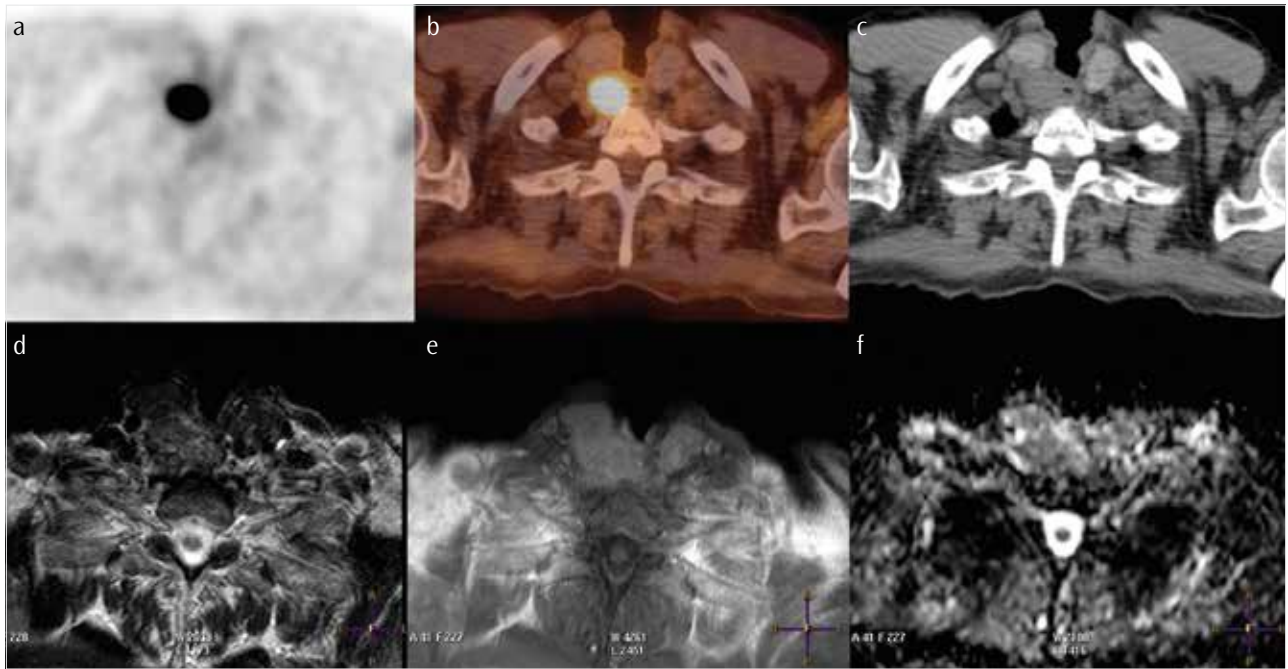


Figure 1. a-f. Transverse FDG-PET/CT and MR images of a 70-year-old patient with a laryngeal tumor following radiotherapy. PET (a), fused PET/CT (b), and low-dose CT demonstrate a positive focus (SUV_{max} value=15.9). T2WI (d) and post-contrast T1WI (e) show a heterogeneously enhanced lesion. The ADC map (f) demonstrates a low signal intensity at the site of the lesion with a mean ADC_{mean} value of $0.72 \times 10^{-3} \text{ mm}^2/\text{s}$. The biopsy revealed the recurrence of the tumor
 FDG-PET/CT: fluorodeoxyglucose positron emission tomography; SUVmax: maximum standardized uptake value; MR: magnetic resonance; ADC: apparent diffusion coefficient; WI: weighted image

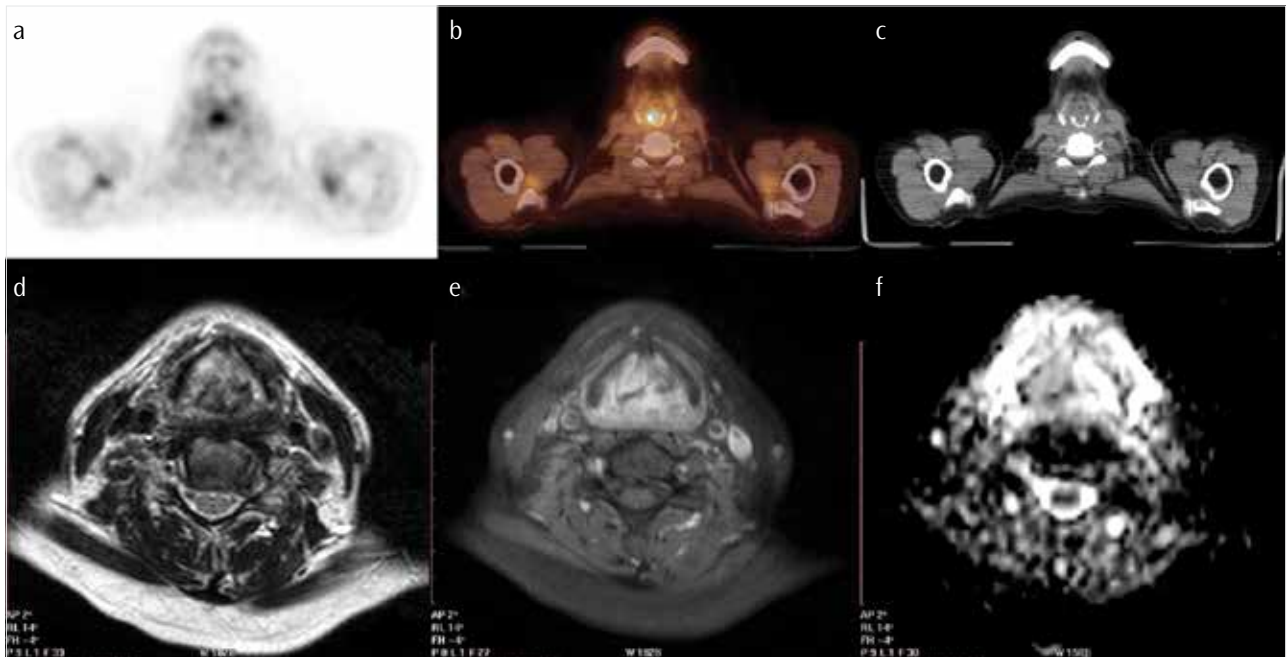


Figure 2. a-f. Transverse FDG-PET/CT and MR images of a 55-year-old patient with a laryngeal tumor after radiotherapy. PET (a), fused PET/CT (b) and low-dose CT demonstrates a positive focus (SUV_{max} value=5). T2WI (d) and post-contrast T1WI (e) show an ill-defined, heterogeneous enhanced lesion. The ADC map (f) shows low signal intensity at the site of the lesion with a mean ADC_{mean} value of $1.60 \times 10^{-3} \text{ mm}^2/\text{s}$. The biopsy revealed post-treatment changes
 FDG-PET/CT: fluorodeoxyglucose positron emission tomography; SUVmax: maximum standardized uptake value; MR: magnetic resonance; ADC: apparent diffusion coefficient; WI: weighted image

calculation of ADC_{mean} values. ADC_{mean} measurements were calculated on ADC maps that were generated from a DW-MRI with a standard b value of 1000 s/mm^2 . We used an ROI with a median size of 30 mm^2 (range: $7\text{--}291 \text{ mm}^2$) to calculate ADC_{mean} values on ADC maps. We measured three ROIs with a size similar to the solid

portion of the mass to obtain the mean ADC_{mean} value corresponding to the contrast-enhanced T1-weighted images that were used to eliminate the effect of possible distortion due to susceptibility artifacts. Furthermore, to avoid necrosis or cystic parts of the tumors, measurements of ADC were illustrated on the corresponding T2-weighted images (Figures 1, 2).

Table 1. Clinical and radiological data of the 23 patients with post-treatment head and neck squamous cell carcinoma

Number	Age (year)	Sex	Location	RT-MRI time (day)	RT-PET/CT time (day)	MRI-PET/CT time (day)	Mean ADC _{mean} ($\times 10^{-3}$ mm ² /s)	SUV _{max}	Recurrence
1	76	M	Oral cavity	57	65	8	0.84	6.7	-
2	49	M	Nasopharynx	74	77	3	1.267	4.1	-
3	55	M	Larynx	88	95	7	1.349	3.69	-
4	52	M	Nasopharynx	68	73	5	1.701	4.7	-
5	55	F	Larynx	43	44	1	1.601	5	-
6	54	M	Oral cavity	62	65	3	1.81	5.1	-
7	49	M	Larynx	52	61	9	0.847	7.6	-
8	69	M	Larynx	71	77	6	2.727	2.1	-
9	74	M	Larynx	65	69	4	3.366	1.8	-
10	65	M	Larynx	83	90	7	0.867	6.2	-
11	64	M	Larynx	44	53	9	1.098	2.6	-
12	19	F	Oral cavity	74	75	1	0.852	15	+
13	63	M	Larynx	92	99	7	0.737	7.9	+
14	70	M	Larynx	53	62	9	0.721	15.9	+
15	69	M	Larynx	65	71	6	0.783	16.5	+
16	74	M	Larynx	64	68	4	0.709	9.7	+
17	70	M	Larynx	98	103	5	0.678	26.5	+
18	81	F	Oral cavity	61	69	8	0.948	26.3	+
19	67	M	Nasopharynx	77	89	12	0.915	25	+
20	81	M	Larynx	71	76	5	0.677	16.5	+
21	65	M	Larynx	83	90	7	0.867	6.2	+
22	71	M	Larynx	80	92	12	0.71	14.1	+
23	53	M	Oral cavity	92	93	1	0.674	8.1	+

RT-MRI and RT-PET/CT time indicate the delay times between radiotherapy and MRI. FDG PET/CT imaging; MRI-PET/CT time, delay time between the two examinations
 SCC: squamous cell carcinoma; RT: radiotherapy; MRI: magnetic resonance imaging; PET/CT: positron emission tomography/computed tomography; FDG: fluorodeoxyglucose; ADC: indicates apparent diffusion coefficient; SUVmax: maximum standardized uptake value

SUV_{max} values were automatically calculated with a computer program included in the Philips Extended Brilliance Workspace (version 4.5.3.40140; Philips Medical Systems). SUV_{max} was the maximum tissue concentration of FDG in the ROI. An ROI was placed with the aid of contrast-enhanced T1-weighted and T2-weighted images that were used to identify the same anatomical level of the DW-MRI.

Statistical analysis

Statistical Package for the Social Sciences 19.0 (SPSS Inc.; Chicago, IL, USA) was used for statistical analysis. Descriptive statistics of the continuous variables are presented as the mean, standard deviation, median, minimum, and maximum values. Categorical variables are presented as frequencies and percentages. The Shapiro–Wilk test and graphical techniques, such as histograms, Q–Q, and P–P plots, were used as tests of normality. A Mann–Whitney U-test was used for non-parametric two-group comparisons. Receiver operating characteristic (ROC) analysis was used to determine the cutoff value for post-treatment changes, recurrence discrimination, and comparisons of the area under the curve (AUC) of the SUV_{max} and ADC_{mean}. For all statistical comparisons, a p value of <0.05 was considered to be statistically significant.

Results

According to the pathological diagnosis and clinical and radiological follow-up, recurrence was detected in 12 patients, and post-treatment changes were found in 11 patients. Table 1 presents

the raw data of patients. Otherwise, no significant difference was observed in the mean age, mean ROI size, and mean interval from completion of radiotherapy to post-treatment imaging between the recurrence group and the group with post-treatment changes.

ADC_{mean} values recorded in the 12 patients with recurrence ranged from 0.67 to 0.95 $\times 10^{-3}$ mm²/s. ADC_{mean} values noted in the 11 patients with post-treatment changes ranged from 0.84 to 3.37 $\times 10^{-3}$ mm²/s. The median ADC_{mean} values in the patients with recurrence were significantly lower than those in the patients with post-treatment changes (0.73 vs. 1.35 $\times 10^{-3}$ mm²/s, respectively; p<0.001) (Figure 3a).

SUV_{max} values of the patients with recurrence ranged from 6.2 to 26.5, and those of the patients with post-treatment changes ranged from 1.8 to 7.6. The mean SUV_{max} values in the patients with recurrence were significantly higher than those in the patients with post-treatment changes (15.45 vs. 4.70, respectively; p<0.001) (Figure 3b).

The cutoff value for ADC_{mean} to discriminate recurrence and post-treatment changes was 0.95 $\times 10^{-3}$ mm²/s and was statistically significant (p<0.001) with AUC=0.924 (0.734–0.990). The sensitivity, specificity, and accuracy of the cutoff value were 100% (73.4–100.0), 72.73% (39.1–93.7), and 86.96%, respectively. The DW-MRI

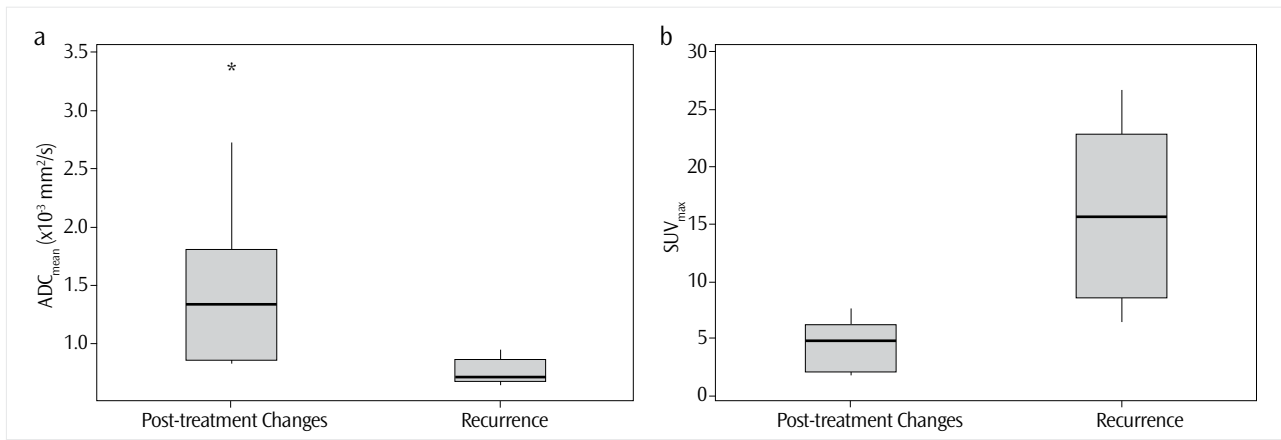


Figure 3. a, b. Box-and-whisker plots of the ADC_{mean} (a) and SUV_{max} (b) values for post-treatment changes and recurrence groups

with a $0.95 \times 10^{-3} \text{ mm}^2/\text{s}$ cutoff value for ADC_{mean} had a 100% negative predictive value (NPV) and 82% positive predictive value (PPV).

The cutoff value for SUV_{max} to discriminate between recurrence and post-treatment changes was 7.6, and it was statistically significant ($p < 0.001$) with an $AUC = 0.981$ (0.818–0.984). The sensitivity, specificity, and accuracy of the cutoff value were 91.67% (61.5–98.6), 100.0% (71.3–100.0), and 91.30%, respectively. The PET-CT with a 7.6 cutoff value for SUV_{max} had a 91% NPV and 92% PPV.

There was no statistical difference between the AUC values of SUV_{max} and ADC_{mean} ($p = 0.342$). However, a moderate negative correlation was found between ADC_{mean} and SUV_{max} values of the patients in the post-treatment changes group ($r = -0.691$; $p = 0.019$). However, there was no significant correlation between ADC_{mean} and SUV_{max} values of the patients in the recurrence group ($r = 0.341$; $p = 0.278$).

Discussion

Both DW-MRI and PET-CT had the ability to diagnose recurrence with a high degree of accuracy, and there was no statistically significant difference between the diagnostic performances of these methods in the same patients ($p = 0.342$). However, DW-MRI had higher NPV than did PET-CT. According to our findings, a diagnosis of post-operative changes can be placed on lesions with an ADC value of > 0.95 via DW-MRI. The occurrence of post-treatment changes combined with recurrence in lesions with ADC values of < 0.95 decreases the PPV of DW-MRI relative to that of PET-CT. According to our results, lesions with SUV values of > 7.6 can be easily accepted as recurrence. Based on these results, we recommend that the first imaging method of choice for post-treatment follow-up of HNSCC patients should be DW-MRI because, compared with PET-CT, it has a lower cost and does not involve ionizing radiation. Imaging with a PET-CT should be chosen as an imaging method for lesions evaluated in DW-MRI as recurrence. This will decrease unnecessary exposure of patients to radiation during follow-up and will also decrease costs.

Our cutoff value of ADC_{mean} for recurrent HNSCC was lower than that of previous studies. Abdel Razeq et al. (4) reported that when $1.30 \times 10^{-3} \text{ mm}^2/\text{s}$ was used as the cutoff value of ADC, differentiation of recurrence from post-treatment changes was made with 87% accuracy, 84% sensitivity, 90% specificity, 94% PPV, and 76%

NPV. Hwang et al. (2) also reported that the optimal cutoff value for ADC_{1000} was $1.46 \times 10^{-3} \text{ mm}^2/\text{s}$ with a 85.0% sensitivity, 84.6% specificity, and 84.8% accuracy. Vogel et al. (1) reported that a threshold value of $1.3 \times 10^{-3} \text{ mm}^2/\text{s}$ for ADC had 74% accuracy, 78% sensitivity, and 71% specificity to distinguish recurrence from post-treatment changes. In these studies, the time intervals between treatment and imaging were also very heterogeneous and highly variable.

This finding may be related to the interval between treatment and imaging, as well as the selection of sampling areas for the calculation of ADC values. Additionally, artifacts caused by air or dentures on the DW-MRI in the upper aerodigestive tract or oral cavity make it difficult to identify small lesions. Occasionally, these artifacts could make it difficult to accurately measure the precise ADC value of the lesions. Therefore, the proper choice of ROI areas during ADC measurement is also a very important factor to decrease false results and observer dependence. Micronecrosis and hypervascular portions in the tumors cause increasing ADC values (8). The areas of gross necrosis and possible areas of edema should be excluded from the ROI, and multiple ROIs with a mean value should be used to prevent sampling error even if the lesion shows significant signal intensity homogeneity or heterogeneity. However, volume averaging and areas of micronecrosis cannot be avoided during ADC measurements (4).

In the present study, in line with the literature, PET-CT exhibited high sensitivity and specificity. In a recent review of diagnostic performance of post-treatment FDG PET or FDG PET/CT imaging in head and neck cancers, Gupta et al. (12) reported that the pooled sensitivity and specificity for detecting residual disease at the primary site was 79.9% (95% CI: 73.7%–85.2%) and 87.5% (95% CI: 85.2%–89.5%), respectively; the review included a total of 24 studies involving 1122 patients. The optimal cutoff value of SUV_{max} was found to be 7.6 in our study. Nakajo et al. (11) reported that the optimal cutoff value to differentiate between disease-free and non-free patients was 12.1 for SUV_{max} with 90% (9/10) sensitivity and 75% (12/16) specificity in the follow-up of 26 patients with primary HNSCC. The SUV_{max} cutoff value in our study was thus lower than previously reported. The reason for this discrepancy may be that a large number of factors affect SUV measurements; these factors principally consist of biological factors such as body size, blood glucose levels, and patient breathing, as well as technological factors including interscanner variability, image reconstruction parameters, injected radioactivity, and the use of CT contrast material (13).

Examining the relationship between SUV_{max} and ADC_{mean} values revealed a moderate negative correlation between these values in the post-treatment changes group ($r=-0.691$, $p=0.019$). In the recurrence group, however, there was no correlation. In the study by Nakajo et al. (11) SUV_{max} and ADC values of primary HNSCC had a negative correlation. According to Nakajo et al., the moderate and inverse correlation demonstrates that glycolytic activity is partially, but significantly, associated with the microstructural environment in HNSCC, Choi et al. (8) showed no significant correlation between SUV_{max} and ADC_{mean} in 47 patients with primary HNSCC. Therefore, the negative correlation in the post-treatment group may be related to the small number of viable cells and increased extracellular water component. In the recurrence group, the microstructural environment that includes microscopic necrotic areas still affects the ADC_{mean} value to a degree. SUV_{max} values depend on the number of viable tumor cells and their metabolic activity and are not as affected by the microstructural environment to the same extent as ADC_{mean} values.

Our study has some limitations: 1) we enrolled a small number of patients from a single center and performed retrospective analysis, which could lead to selection bias. We attempted to include all patients who met the inclusion criteria to minimize selection bias; 2) the time of post-treatment imaging. Edema, active inflammatory reactions, and increased vascular permeability are the major changes after radiation therapy, especially during the first 6 months (14). Therefore, the optimum timing for post-treatment imaging is 12 weeks or more after the completion of radiotherapy (12). In this study, the time of post-treatment imaging was as early as 43 days (range: 43–103 days) in some patients. Patients with early post-treatment imaging were considered to be early recurrence after the endoscopic examination and underwent both DW-MRI and PET-CT. This was one of the reasons for early post-treatment imaging. Additionally, we included HNSCC in various locations with radiotherapy being the last treatment modality, and some of the included patients had also been treated with chemotherapy and surgery.

Our study revealed that PET/CT and DW-MRI are effective methods for distinguishing the recurrence of HNSCC from post-treatment changes, and they have similar and highly accurate results. When both DW-MRI and PET-CT are performed, they offer complementary information and guarantee a complete evaluation of recurrence in HNSCCs. Follow-up should begin with DW-MRI, and in patients with a suspicion of recurrence, PET-CT should be added to the follow-up protocol. Finally, our findings indicate that a combination of DWI and PET means that FDG-PET/MRI may be a more useful method for the diagnosis and follow-up of head and neck carcinoma.

Ethics Committee Approval: Ethics committee approval was received for this study from Bulent Ecevit University Clinical Research Ethics Committee.

Informed Consent: Informed consent was obtained from patients who participated in this study.

Peer-review: Externally peer-reviewed.

Author Contributions: Concept - İ.İ.Ö., İ.Ş.; Design - İ.İ.Ö., Y.S.S.; Supervision - O.E., A.E.D.; Data Collection and/or Processing - İ.İ.Ö., R.U., M.D., İ.Ş.; Analysis and/or Interpretation - M.Ç.B., İ.İ.Ö.; Literature Review - İ.İ.Ö., Y.S.S., M.D.; Writing - İ.İ.Ö., İ.Ş.; Other - O.E., A.E.D.

Conflict of Interest: No conflict of interest was declared by the authors.

Financial Disclosure: The authors declared that this study has received no financial support.

Etik Komite Onayı: Bu çalışma için Bulent Ecevit Üniversitesi Klinik Araştırmalar Etik Kurulu'dan etik komite onayı alınmıştır.

Hasta Onamı: Hasta onamı bu çalışmaya katılan hastalardan alınmıştır.

Hakem Değerlendirmesi: Dış bağımsız.

Yazar Katkıları: Fikir - İ.İ.Ö., İ.Ş.; Tasarım - İ.İ.Ö., Y.S.S.; Denetleme - O.E., A.E.D.; Veri Toplanması ve/veya İşlemesi - İ.İ.Ö., R.U., M.D., İ.Ş.; Analiz ve/veya Yorum - M.Ç.B., İ.İ.Ö.; Literatür Taraması - İ.İ.Ö., Y.S.S., M.D.; Yazıyı Yazan - İ.İ.Ö., İ.Ş.; Eleştirel İnceleme - O.E., A.E.D.

Çıkar Çatışması: Yazarlar çıkar çatışması bildirmemişlerdir.

Finansal Destek: Yazarlar bu çalışma için finansal destek almadığını belirtmiştir.

References

1. Tshering Vogel DW, Zbaeren P, Geretschlaeger A, Vermathen P, De Keyzer F, Thoeny HC. Diffusion-weighted MR imaging including bi-exponential fitting for the detection of recurrent or residual tumour after (chemo)radiotherapy for laryngeal and hypopharyngeal cancers. *Eur Radiol* 2013; 23: 562-9. [CrossRef]
2. Hwang I, Choi SH, Kim YJ, Kim KG, Lee AL, Yun TJ, et al. Differentiation of recurrent tumor and posttreatment changes in head and neck squamous cell carcinoma: application of high b-value diffusion-weighted imaging. *AJNR Am J Neuroradiol* 2013; 34: 2343-8. [CrossRef]
3. Abgral R, Querellou S, Potard G, Le Roux PY, Le Duc-Pennec A, Marianovski R, et al. Does 18F-FDG PET/CT improve the detection of posttreatment recurrence of head and neck squamous cell carcinoma in patients negative for disease on clinical follow-up? *J Nucl Med* 2009; 50: 24-9. [CrossRef]
4. Razeq AAKA, Kandeel AY, Soliman N, El-Shenshawy HM, Kamel Y, Nada N, et al. Role of diffusion-weighted echo-planar MR imaging in differentiation of residual or recurrent head and neck tumors and posttreatment changes. *American journal of neuroradiology* 2007; 28: 1146-52. [CrossRef]
5. Razeq AA. Diffusion-weighted magnetic resonance imaging of head and neck. *J Comput Assist Tomogr* 2010; 34: 808-15. [CrossRef]
6. Thoeny HC, De Keyzer F, King AD. Diffusion-weighted MR imaging in the head and neck. *Radiology* 2012; 263: 19-32. [CrossRef]
7. Payne KF, Haq J, Brown J, Connor S. The role of diffusion-weighted magnetic resonance imaging in the diagnosis, lymph node staging and assessment of treatment response of head and neck cancer. *Int J Oral Maxillofac Surg* 2015; 44: 1-7. [CrossRef]
8. Choi SH, Paeng JC, Sohn CH, Pagsisihan JR, Kim YJ, Kim KG, et al. Correlation of 18F-FDG uptake with apparent diffusion coefficient ratio measured on standard and high b value diffusion MRI in head and neck cancer. *J Nucl Med* 2011; 52: 1056-62. [CrossRef]
9. Varoquaux A, Rager O, Lovblad KO, Masterson K, Dulguerov P, Ratib O, et al. Functional imaging of head and neck squamous cell carcinoma with diffusion-weighted MRI and FDG PET/CT: quantitative analysis of ADC and SUV. *Eur J Nucl Med Mol Imaging* 2013; 40: 842-52. [CrossRef]
10. Burger IA, Huser DM, Burger C, von Schulthess GK, Buck A. Repeatability of FDG quantification in tumor imaging: averaged SUVs are superior to SUV_{max} . *Nucl Med Biol* 2012; 39: 666-70. [CrossRef]
11. Nakajo M, Nakajo M, Kajiya Y, Tani A, Kamiyama T, Yonekura R, et al. FDG PET/CT and diffusion-weighted imaging of head and neck squamous cell carcinoma: comparison of prognostic significance between primary tumor standardized uptake value and apparent diffusion coefficient. *Clin Nucl Med* 2012; 37: 475-80. [CrossRef]
12. Gupta T, Master Z, Kannan S, Agarwal JP, Ghosh-Laskar S, Rangarajan V, et al. Diagnostic performance of post-treatment FDG PET or FDG PET/CT imaging in head and neck cancer: a systematic review and meta-analysis. *Eur J Nucl Med Mol Imaging* 2011; 38: 2083-95. [CrossRef]
13. Adams MC, Turkington TG, Wilson JM, Wong TZ. A systematic review of the factors affecting accuracy of SUV measurements. *American Journal of Roentgenology* 2010; 195: 310-20. [CrossRef]
14. Nömayr A, Lell M, Sweeney R, Bautz W, Lukas P. MRI appearance of radiation-induced changes of normal cervical tissues. *Eur Radiol* 2001; 11: 1807-17. [CrossRef]